

# Online Research @ Cardiff

This is an Open Access document downloaded from ORCA, Cardiff University's institutional repository: <https://orca.cardiff.ac.uk/id/eprint/127358/>

This is the author's version of a work that was submitted to / accepted for publication.

Citation for final published version:

Obaid, Zeyad Assi, Muhssin, Mazin T. and Cipcigan, L. M. ORCID: <https://orcid.org/0000-0002-5015-3334> 2020. A model reference-based adaptive PSS4B stabilizer for the multi-machines power system. Electrical Engineering 102 , pp. 349-358. 10.1007/s00202-019-00879-6 file

Publishers page: <http://dx.doi.org/10.1007/s00202-019-00879-6>  
<<http://dx.doi.org/10.1007/s00202-019-00879-6>>

Please note:

Changes made as a result of publishing processes such as copy-editing, formatting and page numbers may not be reflected in this version. For the definitive version of this publication, please refer to the published source. You are advised to consult the publisher's version if you wish to cite this paper.

This version is being made available in accordance with publisher policies.

See

<http://orca.cf.ac.uk/policies.html> for usage policies. Copyright and moral rights for publications made available in ORCA are retained by the copyright holders.



# A Model Reference -based Adaptive PSS4B Stabilizer for the Multi-Machines Power System

Zeyad Assi Obaid<sup>a</sup>, Mazin T. Muhssin<sup>b</sup>, and L.M. Cipcigan<sup>c</sup>

<sup>a</sup>College of Engineering, University of Diyala  
Baqouba, Diyala, Iraq

<sup>b</sup> Faculty of Engineering, Mustansiriya University  
Baghdad, Iraq

<sup>c</sup>Institute of Energy, School of Engineering, Cardiff University  
Cardiff, Wales, United Kingdom

**Abstract**—Two inputs adaptive IEEE multi-bands power system stabilizer (PSS4B) was developed for oscillations damping control in power systems. Two supplementary loops based on Model Reference (MR) adaptive control were added to the typical PSS4B design. The MR has the same loops' parameters of the typical PSS4B, and hence, avoiding a complex tuning process. The proposed PSS has a self-tuning gain reduction block to avoid any negative impact due to the high gains value during the disturbance time. The proposed PSS was applied on the four machine benchmark power system. To evaluate the robustness of the proposed PSS, it was tested in comparison with the Delta W PSS, one input multi-bands PSS4B (1iMB) and two inputs multi-bands PSS4B (2iMB) stabilizers. The integration of the proposed PSS was demonstrating using different study cases. These cases consider the small signal stability (SSS), large-signal stability (LSS), and the coordination test for the local and inter-area excited power modes. The proposed PSS demonstrated robust and superior responses in all cases.

**Index Terms**—Low-frequency oscillation, Adaptive PSS4B, Self-tuning gains, Model reference adaptive control, multi-inputs multi-bands PSS.

## I. INTRODUCTION

THE design of the Automatic Voltage Regulator (AVR) and the PSS can be coordinated to provide an optimal power stability in term of both transient and oscillation stability analysis [1]. In addition, the actions of both devices are dynamically connected [2]. The PSS is a supplementary controller which provides an additional damping signal to the AVR excitation system to damp the low-frequency oscillation [3]. In wide area interconnected power systems, the inter-area low-frequency oscillations may increase and could affect the security and stability of the large power systems limiting the power flow in the system tie-lines. Therefore, a wide area PSS has a significant impact on tackling this problem, especially with the use of the new Phasor Measurements Units (PMUs) in the modern power systems [4-6]. In addition, the increase of the Renewable Energy Resources (RESs) integration into power systems will lead to a reduction of the system's inertia.

This reduction of inertia impacts the transient stability and the un-damped small signal stability, and hence, inter-area oscillations will be increased [7]. The IEEE Excitation System subcommittee introduced a new model of multi-bands PSS named IEEE PSS4B [8]. This model is designed to deal with a various range of frequencies, and hence, with various range of oscillation modes. The PSS4B has two inputs which are: the rotor speed ( $\Delta\omega$ ) and the electrical power ( $Pe$ ) with two-speed transducers [8]. Also, it has a supplementary loop at each input with different phase compensation and Notch filters [5, 8-11]. A simple tuning procedure for PSS4B is proposed by an IEEE report [12]. The main aims of the tuning procedure are to select three levels of frequencies and associated gains for (i) the low oscillation, (ii) the intermediate oscillation and (iii) the higher oscillations at the stator terminals. The tuning method is implemented using four different equations to obtain the best value of the time constant at each band. Furthermore, the associated gains are set to reasonable values for giving an acceptable contribution of the band amplitude in a wider range of frequencies. Therefore, the frequency response of the total PSS will supply the exciter with more accurate compensation signal.

The Multi-Band PSS4B controller proposed in IEEE® St. 421.5 [15] had the two inputs connected to the ( $\Delta\omega$ ) only and neglect the second input ( $Pe$ ) [16]. However, the low-frequency sensitivity of the electrical power path is important because it measures the response of the PSS to the mechanical power steps and ramps [8]. In addition, considering the two inputs in the PSS controller is widely recommended especially in the case of complex oscillations where two types of oscillation occur [10, 14]. Therefore, the proposed version of PSS4B controller considers both  $\Delta\omega$  and  $Pe$  inputs.

The PSS4B model is new to the market, and only a few relevant papers discussed its design and tuning challenges, highlighting its superior performances in comparison to some older models of PSS [8, 9, 11, 13]. The PSS4B provides an additional degree of freedom to get the robustness and optimal tuning over a wider range of frequency. However, the large number of adjustable parameters of PSS4B may increase the complexity of the tuning process, compared to the PSS2B older

model which has only six parameters. In addition, the second input ( $P_e$ ) introduces a small risk because it has a high-power oscillation which requires a good tuning method. The electric power input is sensitive to the high-frequency noise [8]. Therefore, the proposed multi-bands IEEE PSS4B was designed with an adaptive self-corrections technique and two inputs consideration.

Furthermore, the PSS4B gains with its high value are more aggressive and, therefore, more effective in the inter-area frequencies between 0.1 and 1 Hz [8]. Therefore, the proposed PSS4B controller was designed with an adaptive gain reduction technique to reduce the impact of the high gain during high oscillation value. The main objectives of this paper are:

1. To design a modern two inputs PSS4B with an adaptation mechanism and self-correction technique by using the typical data and structure of the IEEE PSS4B.
2. To demonstrate that the simplicity of the developed design avoids any additional complex tuning process.
3. To demonstrate the performances of the proposed controller on a multi-machines benchmark power system.

## II. THE IEEE PSS4B STABILIZER

The IEEE PSS4B was proposed with two inputs which are: the rotor speed ( $\Delta\omega$ ) and the electrical power ( $P_e$ ) and two-speed transducers [8]. However, as it is mentioned earlier, the second input ( $P_e$ ) introduces a small risk because it has a high power oscillation which requires a good tuning method. Therefore, the PSS4B design proposed in IEEE® St. 421.5 [15] had the two inputs connected to the ( $\Delta\omega$ ) only and neglected the second input ( $P_e$ ) [16] (see Fig. 2). The tuning method presented earlier in [12] aimed to obtain three levels of frequencies, which are: (i) the low oscillation, (ii) the intermediate oscillation and (iii) the higher oscillations at the stator terminals as shown in Fig. 1.

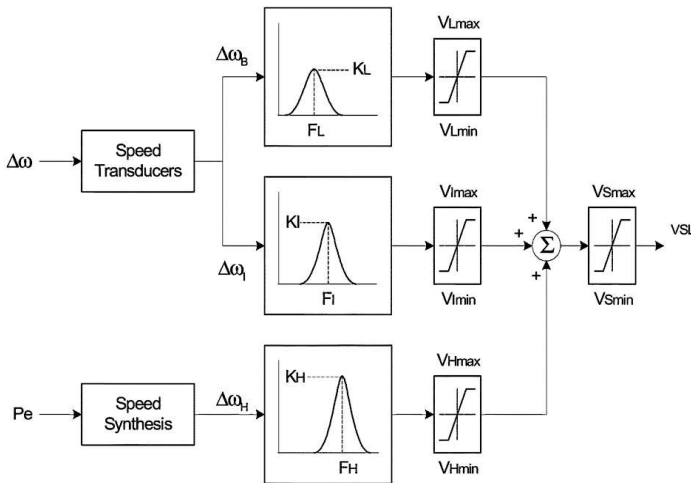


Fig. 1. Block diagram of the PSS4B with its three frequency levels [8].

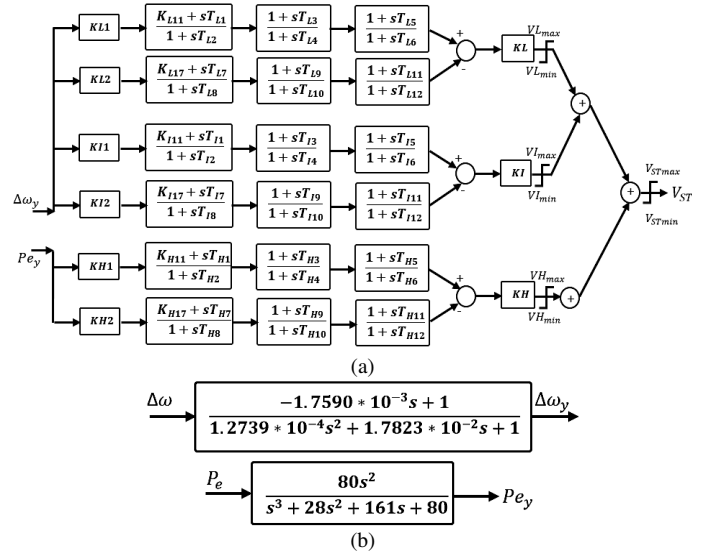


Fig. 2. The PSS4B stabilizer, (a) general layout, and (b) the inputs transducers [8].

The parameters of the PSS4B are shown in Table I with the values according to IEEE® St. 421.5 [15]. The full detail of the design of these parameters are presented in [16]. The values of the parameters can cover a damping for a frequency ranging from 0.04 to 7 Hz [8].

TABLE I  
TIME CONSTANTS AND GAINS VALUE OF THE PSS4B

Frequency Band					
Low (L)		Intermediate (I)		High (H)	
$T_{L1}$	1.667	$T_{I1}$	1	$T_{H1}$	0.01
$T_{L2}$	2	$T_{I2}$	1	$T_{H2}$	0.012
$T_{L3}$	0	$T_{I3}$	0.25	$T_{H3}$	0
$T_{L4}$	0	$T_{I4}$	0.3	$T_{H4}$	0
$T_{L5}$	0	$T_{I5}$	0	$T_{H5}$	0
$T_{L6}$	0	$T_{I6}$	0	$T_{H6}$	0
$T_{L7}$	2	$T_{I7}$	1	$T_{H7}$	0.012
$T_{L8}$	2.4	$T_{I8}$	1	$T_{H8}$	0.0144
$T_{L9}$	0	$T_{I9}$	0.3	$T_{H9}$	0
$T_{L10}$	0	$T_{I10}$	0.36	$T_{H10}$	0
$T_{L11}$	0	$T_{I11}$	0	$T_{H11}$	0
$T_{L12}$	0	$T_{I12}$	0	$T_{H12}$	0
$K_{L11}$	1	$K_{I11}$	0	$K_{H11}$	1
$K_{L17}$	1	$K_{I17}$	0	$K_{H17}$	1
$KL1$	66	$KI1$	66	$KH1$	66
$KL2$	66	$KI2$	66	$KH2$	66
$KL$	9.4	$KI$	47.6	$KH$	233
$VLmax$	0.075	$VImax$	0.15	$VHmax$	0.15
$VSmax = 0.15$					

## III. THE PROPOSED PSS4B STRUCTURE AND DESIGN

The proposed PSS is a developed version of the IEEE PSS4B stabilizer. The proposed design has the full structure, parameters, frequency range, and the layout of the PSS4B presented in section II. The design is a Model Reference/Fuzzy-Based Self-tuning Adaptive PSS4B (MRSAPSS) controller. This model considers both PSS4B inputs which are the  $\Delta\omega$  and  $P_e$ . Additional loops and the automatic gain reduction block were added to the typical PSS4B structure (see Fig.2) to formulate the proposed adaptive design. The loops are based on the Model reference adaptation mechanism [17]. The upper loop is for the Low-Intermediate frequency parts as shown in Fig. 3 with the name of (*Adaptive MR<sub>L+I</sub>*). Another loop was added for the High frequency part as shown in Fig. 3 with the name of (*Adaptive MR<sub>H</sub>*). The Automatic gains reduction



block was integrated in each inputs/output gain as shown in Fig. 3 with the name of (Akji).

#### A. Implementation of the Adaptive MR Loops.

The design is similar to the idea of the MR using the MIT rules [17]. However, the typical structure of the MR cannot be applied directly to the power system [13]. The main goal of the proposed design is to achieve a stable PSS with two inputs and an adaptation mechanism to avoid any risk associated with the consideration of the second input (Pe). The blocks  $MR_H$  and  $MR_{L+I}$  (in Fig.3) represent the MR as supplementary loops for each part of the PSS4B design. However, increasing the blocks in the PSS4B design can increase the complexity of the design. Therefore, the blocks of each loop have similar structure and parameters' value to the Low-Intermediate part (L-I) and High-Frequency (H) part (see Fig.3) from the original PSS4B design (Table I). The equivalent transfer functions of each block ( $MR_{L+I}$  and  $MR_H$ ) according to the IEEE® St. 421.5 [15] were generated in the Matlab/Simulink to complete the design and for obtaining the parameters (presented in Section C). These functions are shown in the state space representation form (Equations 1, and 2). The total  $MR_{L+I}$  model is the summation of the Low model (Equations 3-6) and the Intermediate model (Equations 7-10). The High-frequency model is shown in Equations 11-14.

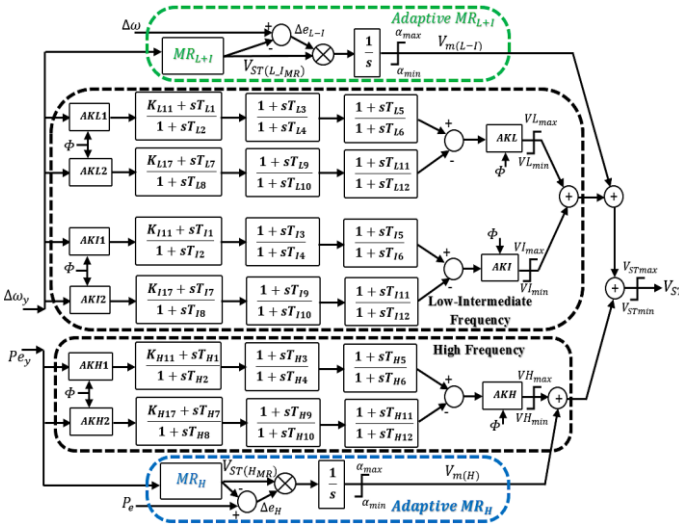


Fig. 3. The general layout of the proposed MRSAPSS.

$$\hat{x} = Ax + Bu \quad (1)$$

$$y = Cx + Du \quad (2)$$

$$A_L = \begin{bmatrix} -0.4167 & 0 \\ 0 & -0.5 \end{bmatrix} \quad (3)$$

$$B_L = \begin{bmatrix} KL1 \\ KL2 \end{bmatrix} \quad (4)$$

$$C_L = [-0.6528 \quad 0.7825] \quad (5)$$

$$D_L = [0.01567] \quad (6)$$

$$A_I = \begin{bmatrix} -1 & 0 & 0 & 0 \\ -1 & -3.333 & 0 & 0 \\ 0 & 0 & -1 & 0 \\ 0 & 0 & -1 & -2.778 \end{bmatrix} \quad (7)$$

$$B_I = \begin{bmatrix} KI1 \\ KI1 \\ KI2 \\ KI2 \end{bmatrix} \quad (8)$$

$$C_I = [-39.67 \quad 26.44 \quad 39.67 \quad -22.04] \quad (9)$$

$$D_I = [1.137e - 13] \quad (10)$$

$$A_H = \begin{bmatrix} -83.33 & 0 \\ 0 & -69.44 \end{bmatrix} \quad (11)$$

$$B_H = \begin{bmatrix} KH1 \\ KH2 \end{bmatrix} \quad (12)$$

$$C_H = [3194 \quad -2662] \quad (13)$$

$$D_H = [-4.547e - 13] \quad (14)$$

The MR mechanism in this design is proposed to calculate the remaining error between the MR's damping output signal and the signals from the generator. If the generators' signals are undamped enough, there will be an error weather is  $\Delta e_H$  or  $\Delta e_{L-I}$  or both of them. This error is then multiplied by the MR output and accumulated to supplement the original PSS4B structure (see Fig.3). To avoid the total PSS's output not to be driven by only the MR loops, the output limiters ( $\alpha_{max}, \alpha_{min}$ , Fig.3) of these loops were set lower than the lowest limiter value in the original PSS, see ( $V_{Lmax}, V_{Lmin}$ ) in Table I.

#### B. Implementation of the Automatic Gains Reduction.

The PSS4B gains with its high value are more aggressive and, therefore, more effective in the inter-area frequencies between 0.1 and 1 Hz [8]. Three different configurations previously assigned when defining the stability: a strong, medium and weak system which is characterized respectively by a small, average and large line reactance [8].

Moreover, higher PSS gains are required in case of local oscillation mode to achieve a desirable performance on a weak grid. However, the high gain has a risk of instability margins in the strong grids [8].

Hence, it is necessary to keep this trade-off in control limits. The proposed gain reduction block is keeping the same value of the typical PSS4B gains in the steady state response and provides a temporary gains value reduction only when the disturbance occurs. The range of this technique is very small avoiding the reduction of the gain value for a long period. The proposed block is based on one Fuzzy Triangle Membership Function (MSF) for all inputs/outputs gains at the same time (see Fig.4-G1).

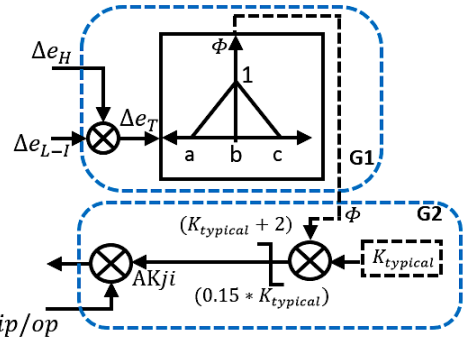


Fig. 4. The general layout of the proposed gain reduction block.

The idea of this mechanism is that when the disturbance occurs, there will be an error ( $\Delta e_H$  or  $\Delta e_{L-I}$ ) or both errors

occurs. The occurred error can be used as an indication for the disturbance, and hence, to trigger the mechanism of this block. The error is processed in the Fuzzy triangular MSF (see Fig.4-G1) to provide the output value ( $\Phi$ ) of the gain reduction. This value is between 0 and 1 and represents the Fuzzy set value range. The  $\Phi$  is then multiplied by the typical value of the input/output gains (Table I) to get the final value of the adaptive gains ( $A_{kji}$ ), see Fig.4-G2. The MSF as shown in G1-Fig.4 was implemented using the Equation (15) as a centralized block in the proposed MRSAPSS. The multiplication process as shown in G2-Fig.4 was implemented at each inputs/outputs gain (see Fig.3).

$$\Phi(\Delta e_T; a, b, c) = \begin{cases} 0 & \Delta e_T \leq a \\ \frac{\Delta e_T - a}{b - a} & a \leq \Delta e_T \leq b \\ \frac{c - \Delta e_T}{c - b} & b \leq \Delta e_T \leq c \\ 0 & c \leq \Delta e_T \end{cases} \quad (15)$$

### C. Obtaining the Optimal Design Parameters.

The proposed design was initially tested and optimized in the linearized model of the single machine model (see Fig. 5 [18, 19]). The model parameters in Fig. 5 were used based on [18]. The Particle Swarm Optimization (PSO) method was considered to obtain the best value of the proposed design parameters. The parameters of a, b, and c in Fig.4-G1, as well as the inputs gains of both MRL+I and MRH (Equations 4, 8, and 12), were considered in this optimization.

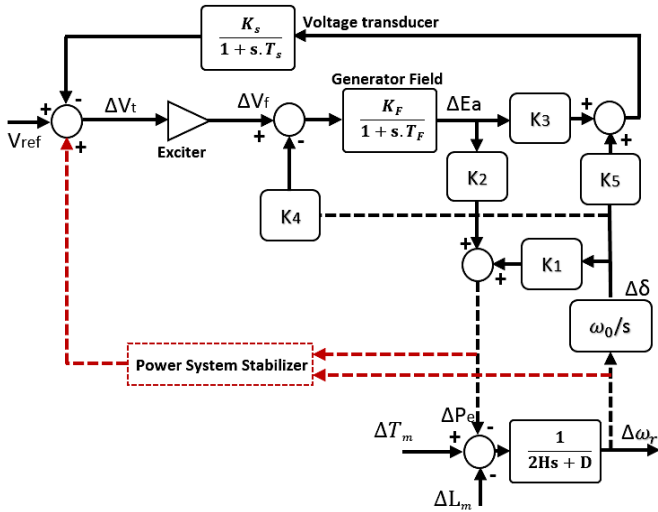


Fig. 5. The Linearized model of the single machine [18].

The optimal values were obtained by minimizing the summation of the total error of the MR loops ( $\Delta e_T$  in Fig. 4 – G1). The Integral Square Error (ISE) function was implemented as a cost function in the optimization process (Equation 16). A disturbance value equal to 0.03 p.u was applied at  $\Delta L_m$  (see Fig. 5) to reach the minimum value of this function and to obtain the optimal values. The optimal value of the inputs gains (KL1, KL2, KI1, KI2, KH1, and KH2) of the MR loops were 10. The rest of the loops' details are similar to the original PSS4B details (Table I). The only difference in there details is in the output limiter ( $V_{ST}$  in Fig. 3) which was reduced to 0.1 instead of 0.15 (see Table I). This proposed value provided the lower deviation value in comparison with 0.15 value considering the proposed PSS. The MSF range parameters a, b, and c (see Fig.4-G1) were obtained and their value is equal to -0.001, 0, and +0.001, respectively.

$$ISE = \sum_{t=0}^{Maxiteration} (\Delta e_T)^2 \quad (16)$$

### IV. SIMULATION RESULTS

The proposed PSS was designed by using a linearized power single machine power system. In order to evaluate the performance of the proposed MRSAPSS control, it is important to validate it in a well-known multi-machines Benchmark power system. Kundur Test system with four machines-two areas [20] (presented in Fig. 6) is widely used in the Dynamic stability assessment [8, 13, 21]. The system has Symmetrical two areas with two machines in each area connected by weak tie-lines. The machines have the same rating equal to 900MVA, 20kV. The nominal voltage of the tie-lines is 230kV. The loads are distributed to allow Area 2 to import about 413MW from Area 1. The system has a complex power system oscillation. Area 1 and Area 2 have local modes equal to 1.12 Hz and 1.16 Hz respectively. The whole system has an Inter-Area mode at a frequency equal to 0.64 Hz [20, 22]. Generators' parameters, loads, Exciters, and tie-lines' parameters are presented in the Appendix based on [13]. **The impact of RES will not be uniform across the wide system. This impact was considered as an inertia reduction, generators G3 and G4 have a lower inertia value than G1 and G2.**

For the performance and robustness evaluation, the proposed MRSAPSS controller was compared with three other PSSs types: (i) the one input Delta W Kundur PSS, (ii) the one input MB-PSS (1iMB) [20] and (iii) the two inputs MB-PSS (2iMB). For a fair comparison, the output limiter of the 2iMB was set to 0.1 similar with the proposed MRSAPSS. All generators were

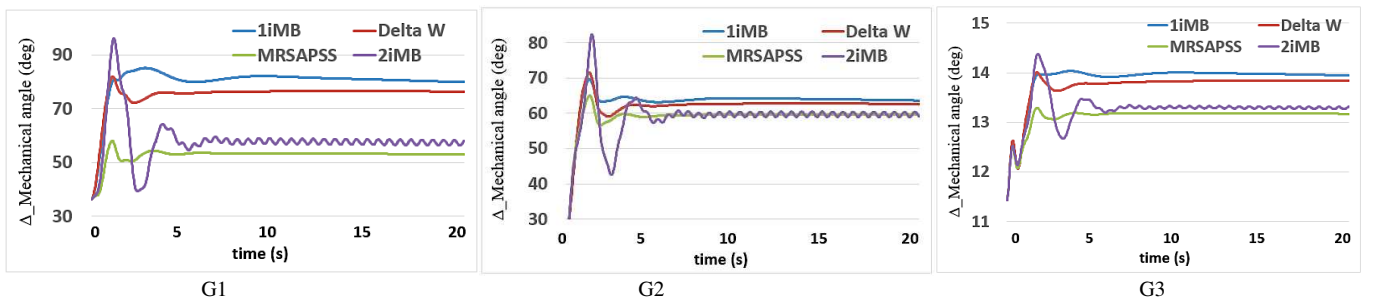


Fig. 11. Machines' mechanical Angle Deviation of generators versus G4 with SSS and replacing only G1's PSS.

assumed to have a Delta W PSS as a base case, and the PSS type was changed only for the generator G1. All simulation results were stored as vectors in Excell files to display the comparison.

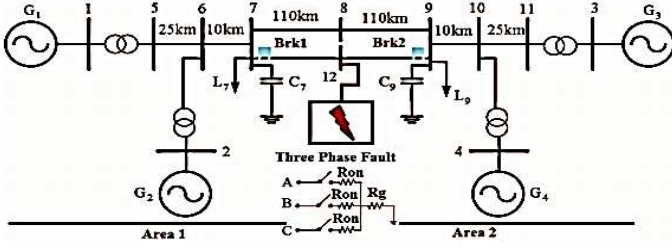


Fig. 6. Two areas- Four Machines Kundur Test System [8, 13, 20, 21].

#### A. Study Case 1: Small Signal Stability Assessment (SSS).

This test was done by applying 12-cycle pulse on voltage reference of G1 [20]. Fig.7-Fig.10 show the Rotor Speed Deviation of the generators. It is clear that adding the proposed MRSAPSS controller to G1 resulted in a great improvement of all generators' response. The 2iMB controller increased the oscillations in G1 and the nearby G2 and provided high overshoot in the generators located at the far end of the network.

Fig.11 shows the mechanical angle deviation of G1, G2, and G3 versus the far end generator G4 ( $\Delta_{\theta}$  versus G4). This comparison is necessary to test the pole-slip between generators. If the pole-slip exceeds 180 degrees, the system has unstable pole slip. The simulation results show that adding the MRSAPSS to G1 increases the stability by reducing the value of  $\Delta_{\theta}$  of all generators. Hence, the system is prevented from falling into unstable pole slip and becomes more secure.

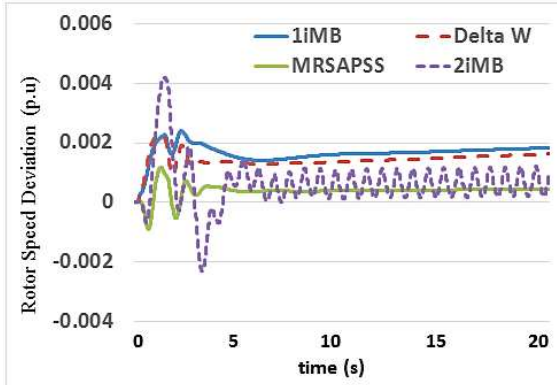


Fig. 7. Machines' Rotor Speed Deviation of G1 with SSS.

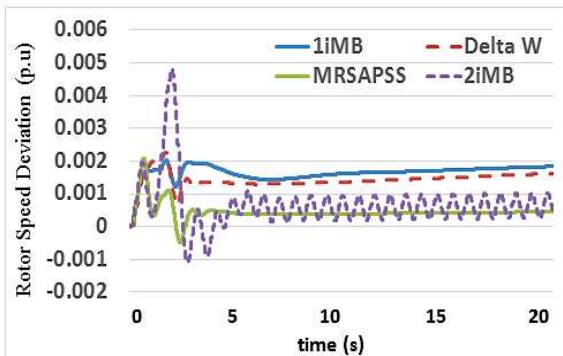


Fig. 8. Machines' Rotor Speed Deviation of G2 with SSS.

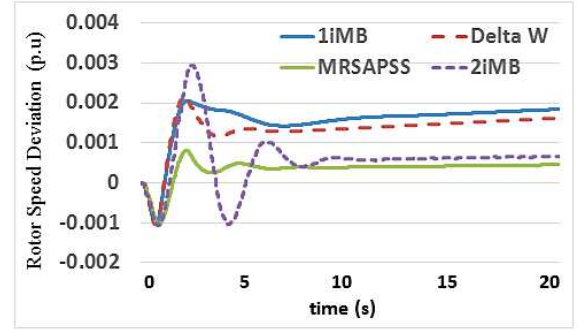


Fig. 9. Machines' Rotor Speed Deviation of G3 with SSS.

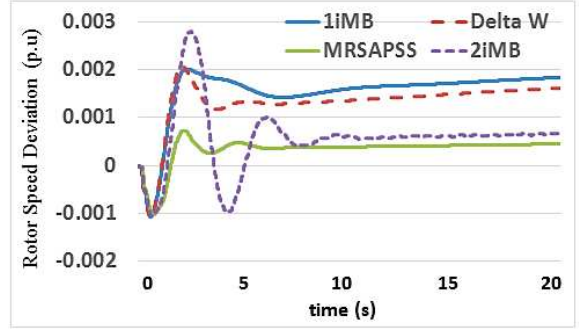


Fig. 10. Machines' Rotor Speed Deviation of G4 with SSS.

#### B. Study Case 2: Large Signal Stability Assessment (LSS).

This test was done by applying an 8-cycle, three-phase fault, with  $R_{on}=0.001\Omega$  and  $R_g=0.001\Omega$  [20] line outage. Small Signal Stability Assessment was applied at the G1 reference voltage as well. These highly stressed conditions are necessary for assessing the PSS when the small signal assessment only is not sufficient. Fig.12-Fig.15 show the Rotor Speed Deviation, and it was found that using the proposed MRSAPSS controller it was achieved a smaller deviation in the rotor speed than with other PSSs. However, there is a small error equal to about -0.0005 p.u. This error is slightly higher than the test with 1iMB and Delta W PSSs controllers and lower than the test with 2iMB controller.

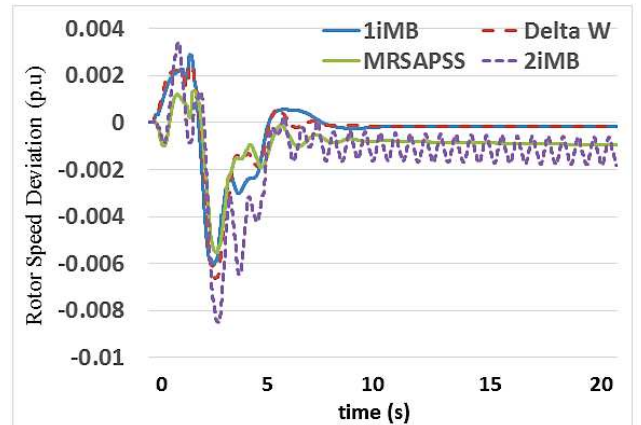


Fig. 12. Machines' Rotor Speed Deviation of G1 with LSS.



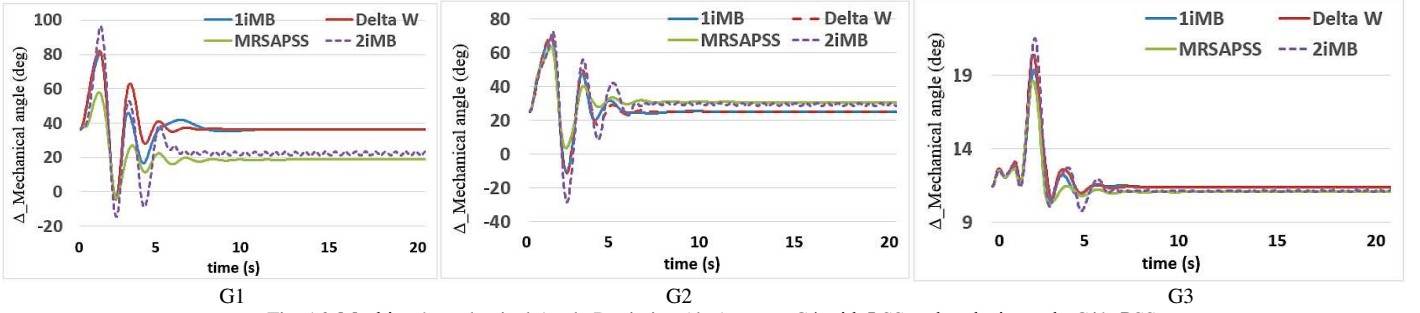


Fig. 16. Machines' mechanical Angle Deviation (deg) versus G4 with LSS and replacing only G1's PSS.

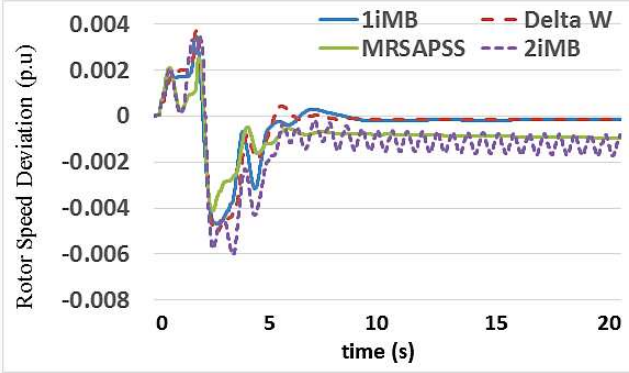


Fig. 13. Machines' Rotor Speed Deviation of G2 with LSS.

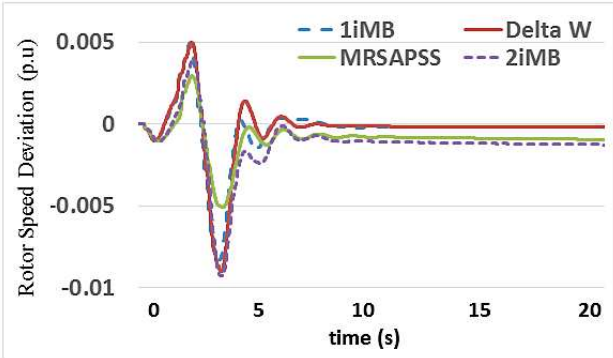


Fig. 14. Machines' Rotor Speed Deviation of G3 with LSS.

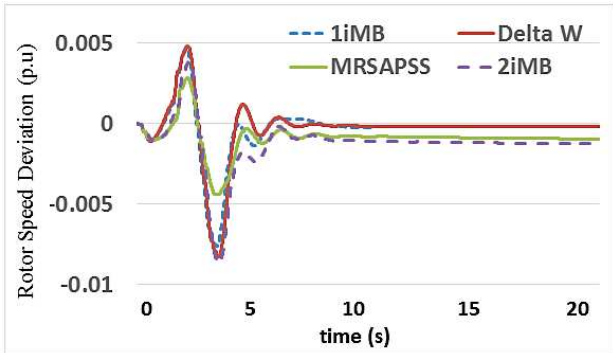


Fig. 15. Machines' Rotor Speed Deviation of G4 with LSS.

Fig. 16 shows the  $\Delta$  theta angle of the machines versus generator G4. The MRSAPSS achieved a lower angle, rotor speed value and deviation in generators G1 and G3, and a lower deviation in generator G2. The angle of the MRSAPSS at G2 was slightly higher than the test with 1iMB and Delta W PSS's controllers in the steady state value of the  $\Delta$  theta.

### C. Study Case 3: Evaluating the Gain Reduction and MR Loops.

For this design, it is necessary to evaluate the performance of the additional structure in the proposed PSS. The gain reduction was included in the proposed design to reduce the trade-off between the needs of considering a high gain or not. Also, the MR upper and lower loops were proposed to tackle the problem of integrating the second input  $P_e$  without the need of any tuning process to the PSS4B. Fig.17-Fig.18 shows a comparison in small signal stability and large-signal stability between different types of controllers: 1iMB, the proposed MRSAPSS, the MRSAPSS without the gains reduction (MRSAPSS1) and the MRSAPSS without MR loops (MRSAPSS2). The effect of the gains reduction has a great impact in the SSS, and it is slightly noticeable in the LSS.

Also, removing the MR loops leads to a behavior similar to the typical 2iMB controller. It was found that both loops are necessary to provide a stable response. Fig. 19 shows the online gains self-tuning in the gain reduction block during the disturbance of SSS. The typical (type.) values for each gain are presented. In Fig.19 can be seen the gains' value reduction process during the disturbance time only.

### D. Study Case 4: Coordination Evaluation.

In order to verify that the proposed PSS does not lead to a lack of coordination, the following tests are performed similarly to what proposed in [13]. The test is done by adding an oscillation with the magnitude of 0.1 p.u. and frequency to the output power of different generators. (a) Local mode of area 1 is excited by adding an oscillation with 0.1 p.u magnitude and a frequency of 1.12 Hz to the Generator 1. (b) Local mode of area 2 is excited by adding an oscillation with 0.1 p.u magnitude and a frequency of 1.12 Hz to the Generator 3. (c) Inter-area mode of the whole system is excited by adding an oscillation with 0.1 p.u magnitude and a frequency of 0.48 Hz to the Generator 1.

Fig. 20- Fig. 22 show the results with the case (a), Fig. 23- Fig. 25 show the results with case (b), and Fig. 26-Fig. 27 show the results with case (c). The proposed PSS (MRSAPSS) shows superior results than the typical two inputs PSS4B (2iMB) in all cases and better than other in most cases.

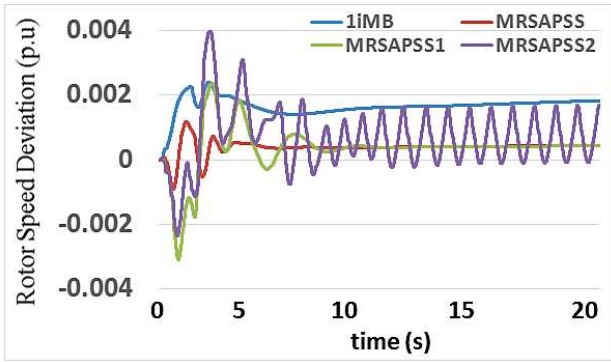


Fig. 17. Rotor Speed Deviation of generator G1 with SSS.

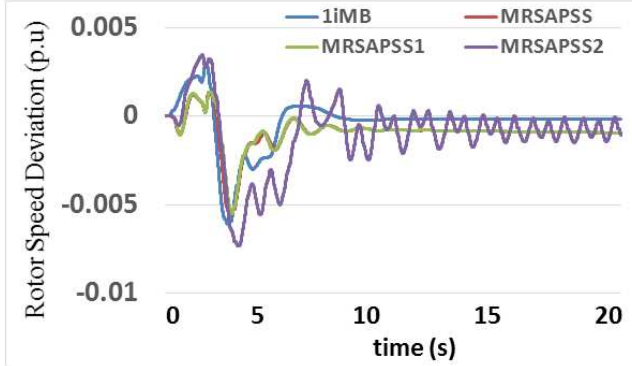


Fig. 18. Rotor Speed Deviation of generator G1 with LSS.

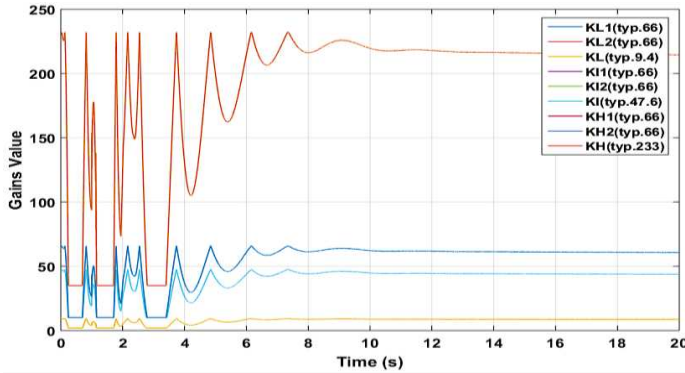


Fig. 19. Self-tuning gains reduction in the developed MRSAPSS controller, during the disturbance of the SSS.

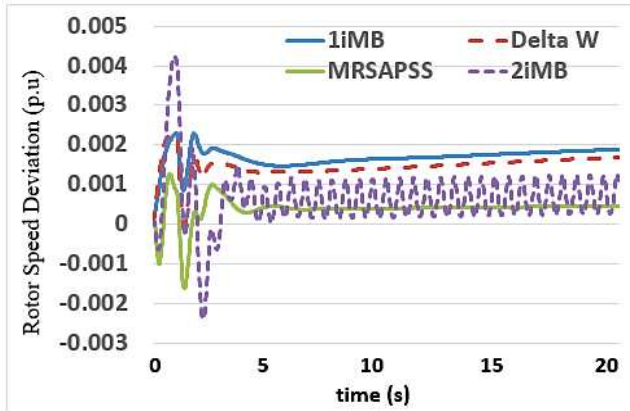


Fig. 20. Rotor Speed Deviation (p.u) of generator G1 with the case a.

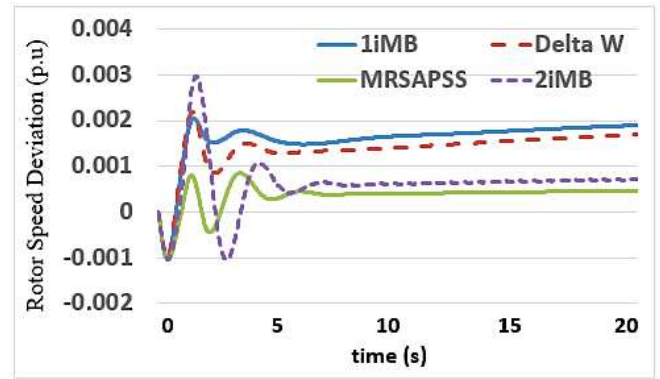


Fig. 21. Rotor Speed Deviation (p.u) of generator G3 with the case a.

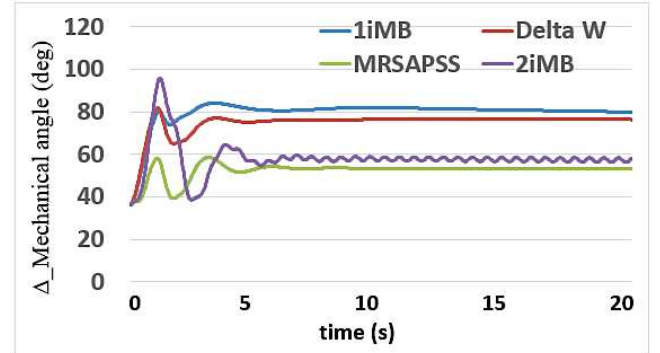


Fig. 22. Mechanical Angle Deviation (deg) of G1 versus G4 with the case a.

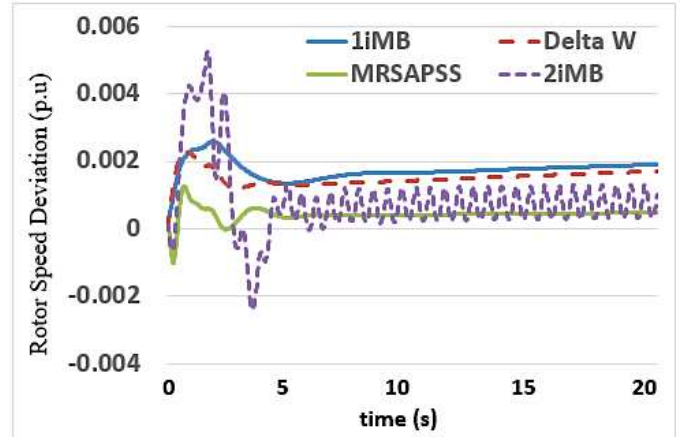


Fig. 23. Rotor Speed Deviation (p.u) of generator G1 with the case b.

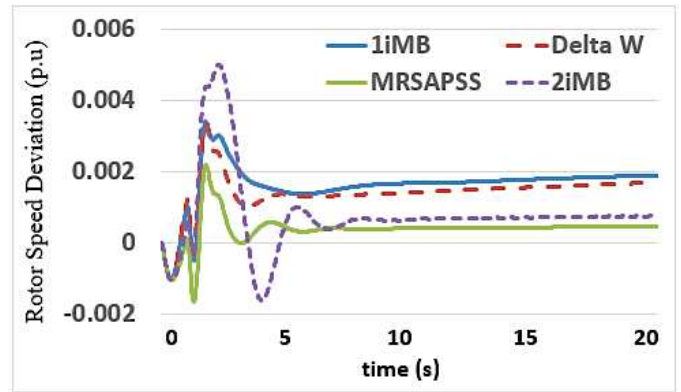


Fig. 24. Rotor Speed Deviation (p.u) of generator G3 with the case b.



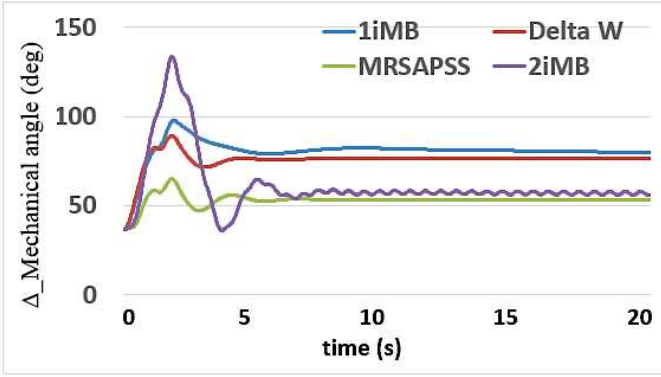


Fig. 25. Mechanical Angle Deviation (deg) of G1 versus G4 with the case b.

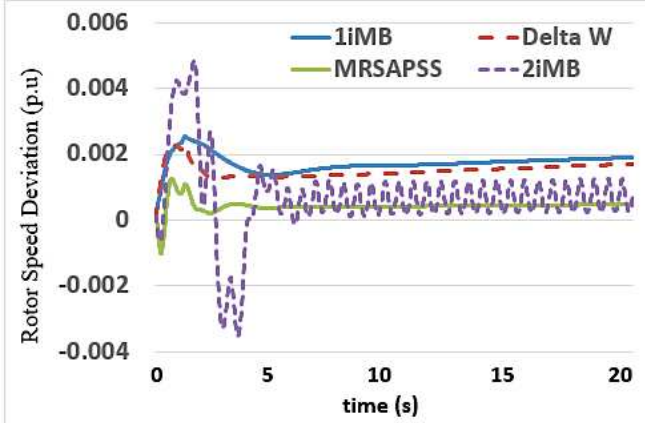


Fig. 26. Rotor Speed Deviation (p.u) of generator G1 with the case c.

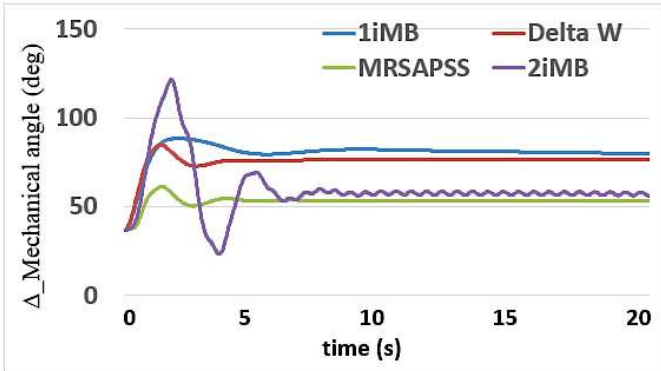


Fig. 27. Mechanical Angle Deviation (deg) of G1 versus G4 with the case c.

## V. CONCLUSION

A developed design of the IEEE PSS4B stabilizer considering both typical inputs are proposed for the control of the oscillatory dynamics in a power system. Two supplementary loops were added to the PSS4B based on the model reference (MR) adaptive control. The MR is represented by the same blocks of the typical PSS4B loops. Hence, no additional parameters' tuning process is required. The gain reduction block is proposed to tackle any trade-off in considering high gains value during the disturbance time. The design is simple, fast and robust against the small signal assessment, large signal assessment, and resonance study cases.

The modern PSSs like the proposed MRSAPSS, and the typical one input PSS4B (1iMB) controller provided good results. These controllers can ensure that there will be no unstable pole slip in the system. However, considering a two

inputs PSS controller has a risk of increasing the oscillation as was demonstrated by using the typical two inputs PSS4B (2iMB) controller. The proposed controller was tested in the Four-machine benchmark power system. Therefore, the proposed design can be a good choice in a network with a complex power system oscillation like the tested network.

## Appendix

### A. Parameters of Kundur Test System

Generator parameters in $pu$					
$X_d$	$X_q$	$X_l$	$X'_d$	$X'_q$	$X''_d$
1.8	1.7	0.2	0.3	0.55	0.25
$X''_q$	$R_a$	$T'_{do}$	$T'_{qo}$	$T''_{do}$	$T''_{qo}$
0.25	0.0025	8.0	0.4	0.03	0.05
$A_{Sat}$	$B_{Sat}$	$\Psi_{T1}$	$H$ ( $G_1$ and $G_2$ )	$H$ ( $G_3$ and $G_4$ )	$D_m$
0.015	9.6	0.9	6.5	6.175	0
Parameters of the lines					
$R$		$X_e$		$b_C$	
0.0001 $pu/km$		0.001 $pu/km$		0.00175 $pu/km$	
Operating point of generating units and loads					
$G_1$	P=700MW, Q=185MVA <sub>r</sub>				
$G_2$	P=700MW, Q=235MVA <sub>r</sub>				
$G_3$	P=719MW, Q=176MVA <sub>r</sub>				
$G_4$	P=700MW, Q=202MVA <sub>r</sub>				
Bus7	$P_L$ =967MW, $Q_L$ =100MVA <sub>r</sub> , $Q_c$ =187MVA <sub>r</sub>				
Bus9	$P_L$ =1767MW, $Q_L$ =100MVA <sub>r</sub> , $Q_c$ =187MVA <sub>r</sub>				

### B. Parameters values of Exciter related to Kundor test system.

full-order exciter						
$k_a$	$k_e$	$k_f$	$K_r$	$T_b$	$V_{r\ min}$	$A_{ex}$
200	1.00	0.001	1.00	0.00	0	0.0056
$T_a$	$T_e$	$T_f$	$T_r$	$T_c$	$V_{r\ max}$	$B_{ex}$
0.001	0.01	0.1	20e-3	0.00	12.3	1.075
reduced-order exciter						
$K_A$	$K_B$	$T_A$	A	B	C	D
200.00	8.5699	0.2595	-3.8530	1.00	643.3739	33.02

## REFERENCES

- [1] A. Dysko, W. E. Leithead, and J. O'Reilly, "Enhanced Power System Stability by Coordinated PSS Design," *Power Systems, IEEE Transactions on*, vol. 25, pp. 413-422, 2010.
- [2] G. J. W. Dudgeon, W. E. Leithead, A. Dysko, J. O'Reilly, and J. R. McDonald, "The Effective Role of AVR and PSS in Power Systems: Frequency Response Analysis," *Power Systems, IEEE Transactions on*, vol. 22, pp. 1986-1994, 2007.
- [3] L. Wenxin, G. K. Venayagamoorthy, and D. C. Wunsch, "A heuristic-dynamic-programming-based power system stabilizer for a turbogenerator in a single-machine power system," *Industry Applications, IEEE Transactions on*, vol. 41, pp. 1377-1385, 2005.
- [4] C. Lin, C. Gang, G. Wenzhong, Z. Fang, and L. Gan, "Adaptive Time Delay Compensator (ATDC) Design for Wide-Area Power System Stabilizer," *Smart Grid, IEEE Transactions on*, vol. 5, pp. 2957-2966, 2014.
- [5] I. Kamwa, S. R. Samantaray, and G. Joos, "Optimal Integration of Disparate C37.118 PMUs in Wide-Area PSS With Electromagnetic Transients," *Power Systems, IEEE Transactions on*, vol. 28, pp. 4760-4770, 2013.
- [6] S. Kamalasadan and G. D. Swann, "A Novel System-Centric Intelligent Adaptive Control Architecture for Damping Interarea Mode Oscillations in Power System," *Industry Applications, IEEE Transactions on*, vol. 47, pp. 1487-1497, 2011.
- [7] N. Grid, "System Operability Framework," 2015.

- [8] I. Kamwa, R. Grondin, and G. Trudel, "IEEE PSS2B versus PSS4B: the limits of performance of modern power system stabilizers," *Power Systems, IEEE Transactions on*, vol. 20, pp. 903-915, 2005.
- [9] J. Lin, G. Xun, X. Ying, X. Huan, W. Tao, S. Weimin, *et al.*, "Application of PSS4B stabilizers in suppressing low frequency oscillations: A case study," in *Power & Energy Society General Meeting, 2015 IEEE*, 2015, pp. 1-5.
- [10] E. D. a. P. G. Committee, "IEEE Guide for Identification, Testing, and Evaluation of the Dynamic Performance of Excitation Control Systems," *IEEE Std 421.2-2014 (Revision of IEEE Std 421.2-1990)*, pp. 1-63, 2014.
- [11] B. Sumanbabu, S. Mishra, K. B. Panigrahi, and G. K. Venayagamoorthy, "Robust tuning of modern power system stabilizers using Bacterial Foraging Algorithm," in *Evolutionary Computation, 2007. CEC 2007. IEEE Congress on*, 2007, pp. 2317-2324.
- [12] "IEEE Recommended Practice for Excitation System Models for Power System Stability Studies," *IEEE Std 421.5-2005 (Revision of IEEE Std 421.5-1992)*, pp. 0\_1-85, 2006.
- [13] A. Yaghooti, M. Oloomi Buygi, and M. H. Modir Shanechi, "Designing Coordinated Power System Stabilizers: A Reference Model Based Controller Design," *Power Systems, IEEE Transactions on*, vol. PP, pp. 1-11, 2015.
- [14] M. E. P. S. S. (PSS), "Power System Stabilizer (PSS)," *New publication, effective*, 2010.
- [15] I. E. Committee, "IEEE recommended practice for excitation system models for power system stability studies," vol. Std 421.5, 2005.
- [16] M. P. S. Stabilizer, "Implement multiband power system stabilizer," *Matlab/Simulink Library, Fundamental Blocks/Machines*, 2015.
- [17] P. J. a. D. M. J. Nigam, "Design of a Model Reference Adaptive Controller Using Modified MIT Rule for a Second Order System," *Advance in Electronic and Electric Engineering*, vol. 3, pp. 477-484, 2013.
- [18] P. Kundur, *Power System Stability and Control*: McGraw-Hill Education, 1994.
- [19] A. Kumar, "Power System Stabilizers Design for Multimachine Power Systems Using Local Measurements," *IEEE Transactions on Power Systems*, vol. 31, pp. 2163-2171, 2016.
- [20] I. Kamwa, "Performance of Three PSS for Interarea Oscillations," in *Sym-PowerSystems Toolbox.*, ed, 2015.
- [21] M. Dobrescu and I. Kamwa, "A new fuzzy logic power system stabilizer performances," in *Power Systems Conference and Exposition, 2004. IEEE PES*, 2004, pp. 1056-1061 vol.2.
- [22] R. R. a. I. Hiskens, "IEEE PES Task Force on Benchmark Systems for Stability Controls-Technical Report," IEEE2015.